

EmoSEM: Segment and Explain Emotion Stimuli in Visual Art

Jing Zhang
hfutzhangjing@gmail.com
Hefei University of Technology
Hefei, China

Zhangbin Li
lizhangbin.mail@gmail.com
Hefei University of Technology
Hefei, China

Dan Guo*
guodan@hfut.edu.cn
Hefei University of Technology
Hefei, China

Meng Wang
eric.mengwang@gmail.com
Hefei University of Technology
Hefei, China

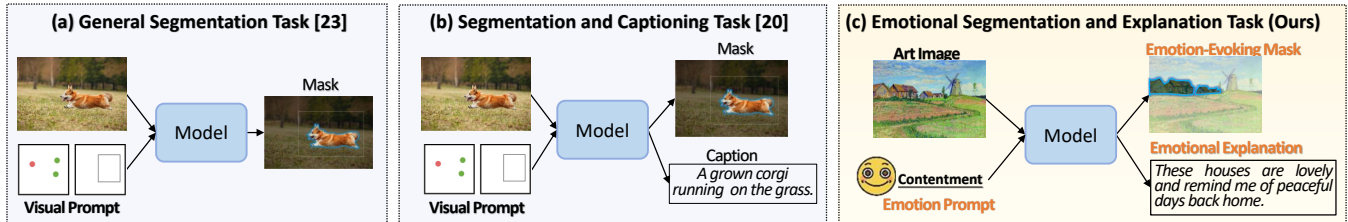


Figure 1: This work focuses on the emotional segmentation and explanation in visual art (c). Given an artistic image, the model generates pixel-level segments (e.g., “house” in dark green mask) that evoke specific emotion (e.g., “contentment”), and provides a textual explanation of how these visual elements elicit such responses. The general segmentation task (a) [23] focuses on segmentation conditioned on visual prompts (e.g., points or boxes), while the segmentation and captioning task (b) [20] enables the model to perform both segmentation and object-oriented captioning. In contrast, without any visual prompts, our work focuses on emotion-oriented stimulus perception and reasoning, which is particularly challenging due to the subjectivity of human emotions and the abstract nature of art.

Abstract

This paper focuses on a key challenge in visual art understanding: given an art image, the model pinpoints pixel regions that trigger a specific human emotion, and generates linguistic explanations for the emotional arousal. Despite the progress of existing research in art understanding, pixel-level emotion understanding still faces a dual challenge: first, the subjectivity of emotion makes it difficult for general segmentation models, such as SAM, to adapt to emotion-oriented segmentation tasks; and second, the abstract nature of art expression makes it difficult for captioning models to balance pixel-level semantic understanding and emotion reasoning. To solve the above problems, this paper proposes the **Emotion Stimuli Segmentation and Explanation Model (EmoSEM)** to endow the segmentation model SAM with emotion comprehension capability. First, to enable the model to perform segmentation under the guidance of emotional intent well, we introduce an emotional prompt with a learnable mask token as the conditional input for segmentation decoding. Then, we design an emotion projector to establish the association between emotion and visual features. Next, more importantly, to address emotion-visual stimuli alignment, we develop a lightweight prefix projector, a module that fuses the learned emotional mask with the corresponding emotion into a unified representation compatible with the language model. Finally, we input the joint visual, mask, and emotional tokens into the language model and output the emotional explanations. It ensures that

the generated interpretations remain semantically and emotionally coherent with the visual stimuli. The method in this paper innovatively realizes end-to-end modeling from low-level pixel features to high-level emotion interpretation, providing the first interpretable fine-grained analysis framework for the field of the artistic emotion computing. Extensive experiments validate the effectiveness of our model. Code will be made publicly available.

CCS Concepts

• **Computing methodologies** → **Computer vision tasks**; • **Applied computing** → **Fine arts**.

Keywords

Art Understanding, Emotional Stimuli Perception, Emotional Explanation

1 Introduction

As early as the 18th century, William James revealed the process of emotion generation, noting that stimuli trigger activity of the autonomic nervous system, which in turn produce an emotional experience in the brain [21]. Visual art generally uses abstract or symbolic visual elements, such as color and composition, to evoke the viewer’s emotions [9]. However, this research remains a major challenge due to the subjectivity of human emotional experience and the abstract nature of art. In this work, we explore a novel and specific emotion understanding problem: given a visual artwork and an emotional prompt, the system detects pixel-level visual

*Corresponding author.

stimuli that evoke human emotional response (e.g., as shown in Fig. 1 (c), the mask of a “houses” corresponding to the emotion “contentment”), and provides a linguistic explanation (e.g., “these houses are lovely and remind me of peaceful days back home”).

In recent years, researchers have been interested in the emotional experience triggered by visual art. Achlioptas *et al.*[1] construct the ArtEmis dataset, containing human emotional choice and associated explanation. Zhang *et al.*[55] develops a small visual language model for art emotion classification and emotion explanation generation. These studies focus on the relationship between holistic image and human emotion. In the corresponding period, Chen *et al.*[6] introduce the APOLO dataset by crowd-sourcing *pixel-level* annotation of emotional stimuli from artworks. However, it focuses exclusively on visual perception by employing a neural network [17] to classify emotions for each pixel of the image. Research on AI-driven art interpretation is still in its early stages. Unlike existing works, our study aims to develop a unified framework capable of both segmenting pixel-level emotional stimuli and generating corresponding explanations, offering a deeper exploration of the intricate connection between visual art and human emotions.

Our task faces two main challenges. Firstly, the general segmentation task focuses on objective semantic segmentation [4, 7, 17, 32, 46, 50, 51, 59], while neglecting emotional aspects. As shown in Fig. 1 (a), the Segment Anything Model (SAM) [23] takes an image and visual prompts (e.g., points, boxes, or masks) as inputs, and outputs semantically relevant masks, e.g., “dog”. It presents strong generalizability to segment anything. However, as shown in Fig. 1 (c), our task does not include any visual prompts; instead, it is guided solely by subjective emotion prompts, making it infeasible to directly adopt the SAM architecture. Secondly, beyond segmenting emotion stimuli, the model should also possess the capability to interpret them. A closely related task is segmentation and captioning. As shown in Fig. 1 (b), the Segment and Caption Anything (SCA) [20] introduces a model that efficiently equip the SAM with the ability to generate regional captions, e.g., “a grown corgi running on the grass”. However, our focus is on the interpretation of emotional stimuli. As illustrated in Fig. 1 (c), the explanation “these houses are lovely and remind me of peaceful days back home” involves not only describing the emotion-evoking mask “houses” but also incorporating the viewer’s emotional experience “remind me of peaceful days back home”. Thus, ensuring alignment between the explanation and both the emotion-evoking mask and the corresponding emotion is another key challenge.

To address the above issues, as illustrated in Fig. 2, we design an Emotion stimuli Segmentation and Explanation Model (EmoSEM) for visual art understanding. 1) First, to fill the gap in segmentation models regarding emotional perception, we introduce an emotional prompt at the input stage of SAM, enabling the model to conduct more precise image segmentation according to emotional requirements. We further design an emotion projector that embeds the emotional prompt into the input feature space of the SAM decoder, which, in conjunction with a learnable mask token and visual information, serves as the input. This ensures that the model enhances the learning and integration of emotional cues while focusing on visual information, thereby achieving more accurate emotion-driven image segmentation. 2) In addition, to enable the language model to provide meaningful emotional explanations for the masks, we

devise a lightweight prefix projector. It transforms the emotional prompt features and the learnable mask token from the SAM decoder into a prefix token. This mapping converts the “emotion-location” intent from the visual task into contextual signals that are interpretable by the language model. Finally, the prefix token is injected at the initial stage of the language model’s decoding process, guiding the model to generate explanations that are not only semantically coherent but also aligned with the emotional cues present in the mask. 3) Besides, inspired by the observation that individuals may perceive different emotions from different regions of an image, we additionally extend our model with a “Multi-Masks” paradigm to simulate the emotional perception of multiple observers simultaneously (refer to Sec. 3.5). It enables concurrent processing of multiple emotion-specific masks, thereby enhancing the flexibility and expressiveness of emotion segmentation.

In summary, our main contributions include:

- We propose an Emotion stimuli Segmentation and Explanation Model (EmoSEM), providing a systematic solution for modeling emotion understanding from low-level perception to high-level cognition.
- We introduce an emotional prompt along with the learnable mask token as input, and design an emotion projector that effectively embeds the emotion prompt into the input space of the segmentation model, addressing the gap in emotion-guided visual segmentation.
- We further develop a simple yet effective prefix projector that products a emotion & mask-aware prefix token to bridge the segmentation model and the language model, facilitating the generation of explanations that are more aligned with emotional stimuli.
- Extensive experiments validate the effectiveness of our model, and showcase its broad applicability across two different paradigms.

2 Related Work

Visual segmentation is a fundamental problem in computer vision, aiming to group pixels of a given image into a set of semantic regions [26]. The field has evolved from CNN-based methods [4, 17, 32, 44, 47] to transformer-based models [7, 50, 59]. Recent works [10, 15, 24, 28, 46, 51] have explored open-world segmentation by using large pre-trained vision language models, such as CLIP [40] or ALIGN [22], to distill or transfer visual-semantic knowledge. In addition, interactive image segmentation has emerged as an important research direction, where the model is required to segment the image according to the user’s interactive information, such as points [27, 52] and bounding boxes [23, 58]. However, all these methods focus on objective segmentation. In this paper, we focus on the subjective and emotionally driven aspects of segmentation, which offers a novel perspective for visual segmentation.

Visual emotion analysis In the affective computing field, “1) **visual emotion recognition**” is a classical task. According to different training objectives, it is divided into emotion classification learning [3, 5, 8, 38] (e.g., positive or negative [2]) and emotion distribution learning [53, 54, 60]. A closely related task to our study is “2) **emotional image captioning**”, which focuses on generating emotionally expressive captions. Many studies [25, 35, 49, 57]

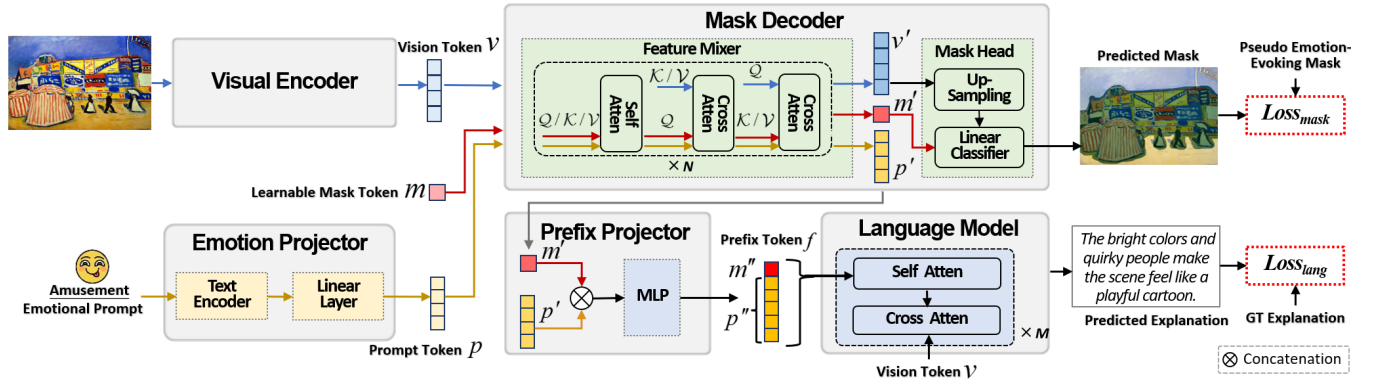


Figure 2: The network of our EmoSEM for emotional segmentation and explanation. It consists of five modules: (a) a visual encoder that extracts features from the input image; (b) an emotion projector that encodes the emotion prompt and embeds it into the semantic space of the mask decoder to facilitate emotion-aware segmentation; (c) the mask decoder that produces pixel-level emotion region predictions by fusing visual and emotional cues with a learnable mask token modeling; (d) a prefix projector that encodes the predicted masks and emotion embeddings into a representation compatible with the language model; and (e) this representation serves as a prefix to guide the language model in generating emotionally grounded interpretations.

aim to incorporate affective words (e.g., “lovely” or “alone”) to sentences. And sarcastic visual captioning [43] and emotional visual dialog [14, 30] have also gained attention. All these methods attempt to enhance the attractiveness and funniness of textual descriptions. In addition, a few studies have explored the “3) *emotional visual explanation*” for art paintings. The dataset ArtEmis [1] and its extended version ArtEmis V2.0 [37] aim to capture the emotions evoked by artworks and the underlying reasons. [55] proposes a small emotional vision language model for both art emotion category and explanation, addressing the balance between model performance and computational complexity. 3) More recently, [6] introduces the task of “4) *emotional stimulus retrieval*” in visual art. It release a dataset, APOLO, which extracts pixel-level annotations of emotional stimuli from artworks through crowd-sourcing, providing a benchmark for the quantitative evaluation of emotional stimulus detection models. However, this work focuses solely on visual cues, without exploring deeper emotion reasoning. For art comprehension, emotional stimulus retrieval and emotional captioning complement each other, with the former identifying “*what*” visual elements trigger emotions, while the latter studying “*how*” these elements influence emotional perception. Building upon this idea, our study develops a unified framework for simultaneously segmenting and interpreting pixel-level emotional stimuli in artworks, establishing new connections between fine-grained visual elements and human emotions.

3 Method

This section presents our EmoSEM, which employs a visual segmentation–language generation pipeline (to be described in Sec 3.1). As shown in Fig. 2, the upper pathway processes the visual input and emotional prompt to generate the emotion-evoking mask (in Sec. 3.2), while the lower pathway converts mask and emotion cues into prefix token that steer a language model to produce emotionally-aligned interpretations (in Sec. 3.3). The multi-task

learning objectives are described in Sec. 3.4. Additionally, we explore different emotion paradigms of EmoSEM in Sec. 3.5.

3.1 Overview for Our Task

Baseline vs. Our Method. The task closely relevant to our study is segmentation and image captioning. SCA [20] is a representative method in this field. It primarily utilizes SAM [23] for image segmentation and a language model [41] for general caption generation. SCA connects the SAM with the language model by introducing a learnable query token q , a learnable mask task token k , and a text feature mixer consisting of a 12-layer stacked bidirectional Transformer[48]. SCA [20] is not inherently designed for our task. To adapt it to our emotion-guided segmentation setting, in Fig. 3 (a), we introduce an emotion prompt along with the learnable token as the input of SAM decoder. And an emotion projector is devised for mapping the emotion prompt into the input feature space of SAM. We term this base model SCA_{base} .

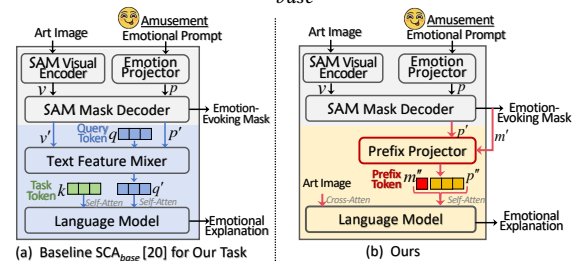


Figure 3: Overview and comparison between the baseline model (a) and the proposed model (b). SCA [20] is not inherently designed for our task; therefore, we construct a baseline model, SCA_{base} (a), upon it. Furthermore, we propose a novel framework, EmoSEM (b), specifically designed to address the challenges of our task.

Our EmoSEM is fundamentally different from the baseline. SCA_{base} follows an *implicit* strategy, primarily relying on the learnable query

token q , which first passes through a deep text feature mixer before being input into the language model for explanation generation (*i.e.*, implicit query context modeling without other cues input for explanation generation). In contrast, EmoSEM adopts an *explicit* design. As illustrated in the yellow box of Fig. 3 (b), we first introduce a lightweight prefix projector that enhances the mask token m' and emotion prompt representation p' into a prefix token aligned with the input space of the language model. Then the learned prefix token together with the art image is fed into the language model for explanation generation (*i.e.*, explicitly utilizing visual, mask, and emotional tokens for explanation generation).

Advancements in EmoSEM include two aspects over the baseline: 1) Subsequent to the mask token output by SAM, with the explicit emotion-mask interaction in the prefix projector, we significantly enhance the expressive ability of emotion prompt token and mask token, making them more emotionally-oriented and informative. 2) Then, the prefix token and the art image are jointly input into the language model, enabling the model to effectively learn the interplay between emotion, the mask, and the visual content, resulting in visually and emotionally aligned explanations.

3.2 Emotional Segmentation

As shown in Fig. 2, it consists of three modules. First, following the SAM architecture [23], we employ a Vision Transformer (ViT) style image encoder [11] as visual encoder E_I . Given an art image I , E_I extracts the visual feature, which is known as vision token, denoted as $v = E_I(I)$. The final spatial shape and feature dimension of visual token v are 64×64 and 256, respectively. In addition, we introduce an emotion projector P_E to map emotional prompt e , *i.e.*, “generate the mask for the emotion ___”, into a suitable representation for the mask decoder. Specifically, we utilize the word embedding layer of the language model [41] as the text encoder to extract a text representation of dimension $l_e \times d_w$, where l_e is the length of e and d_w is the dimension of word embedding. To align the language feature space with the input space of the mask decoder, we further transform the text representation using a linear layer. This process yields an emotional prompt token, formulated as $p = P_E(e) \in \mathbb{R}^{l_e \times d_k}$, where d_k is the feature dimension.

After obtaining the vision token v and emotional prompt token p , we construct a learnable mask token m , which, together with them, is fed into the mask decoder to predict an emotion-evoking mask $\widehat{\mathcal{M}}$. The mask decoder mainly includes a feature mixer and a mask head. The feature mixer is a bidirectional Transformer with N stacked blocks [48]. In each block, the prompt token and the mask token first interact via self-attention (where the concatenation $[p, m]$ is input) to establish emotional and spatial priors, and then engage in bidirectional cross-attention (abbreviated as BiCrossAtt) with the vision token ($[p, m]$ -to- v and vice-versa) to achieve comprehensive cross-modal fusion. The process is formulated as:

$$\text{Blcok}([p, m], v) = \text{BiCrossAtt}(\text{SelfAtt}([p, m]), v), \quad (1)$$

where BiCrossAtt/SelfAtt is implemented by multi-head attention; feed-forward network and residual connection are omitted here. Then, the mask head performs up-sampling on the updated vision token v' , followed by applying an MLP to transform updated mask

token m' into a dynamic linear classifier to predict the foreground probability at each location in the image:

$$\begin{cases} [p', m'], v' = \text{FeatureMixer}([p, m], v) \\ \widehat{\mathcal{M}} = \text{MaskHead}(m', v') \end{cases}, \quad (2)$$

where p', m', v' represent the updated prompt token, mask token and vision token, respectively, and $\widehat{\mathcal{M}} \in \mathbb{R}^{h \times w}$ denotes the predicted emotion-evoking mask. Here, h and w are the height and width of the up-sampled image.

3.3 Emotional Explanation Generation

To effectively integrate emotional and mask information and provide richer contextual cues for the subsequent explanation process, we introduce a prefix projector. This projector is implemented as an MLP network. The updated mask token m' and emotional prompt token p' are concatenated and passed through the MLP network to generate a prefix token f :

$$\begin{pmatrix} p'' \\ \text{(emotional prompt prefix)} \end{pmatrix}, \begin{pmatrix} m'' \\ \text{(mask prefix)} \end{pmatrix} = \text{PrefixProjector}(p', m'), \quad (3)$$

where prefix token $f = [p'', m''] \in \mathbb{R}^{l_f \times d_h}$, and l_f is the length of prefix token; and p'' and m'' are emotional prompt prefix and mask prefix, respectively.

In our case, the GPT-2 [41] is selected as the language model. During training, it takes art image feature v , the prefix token f , and ground-truth explanation \mathcal{X} as input¹, and generates the predicted emotional explanation $\widehat{\mathcal{X}}$. However, GPT2, mainly consists of text-based self-attention layers (where the concatenation $[f, \mathcal{X}]$ serves as input in our work), which is not originally designed for multi-modal inputs. To improve this, we add a cross attention ($[f, \mathcal{X}]$ -to- v) in each block. The process is formulated as:

$$\widehat{\mathcal{X}} = \text{LanguageModel}(v, [f, \mathcal{X}]), \quad (4)$$

where $[f, \mathcal{X}]$ represents the use of the prefix f as the initial input to guide the GPT-2 in generating an explanation that focuses on the emotional aspects and the predicted mask.

3.4 Training Objective

For emotional segmentation, we employ Dice loss [36] to improve segmentation accuracy, and Focal loss [29] to address the foreground-background class imbalance. The training objective for emotional segmentation is as follows:

$$L_{\text{mask}} = L_{\text{Dice}}(\mathcal{M}, \widehat{\mathcal{M}}) + L_{\text{Focal}}(\mathcal{M}, \widehat{\mathcal{M}}), \quad (5)$$

where \mathcal{M} and $\widehat{\mathcal{M}}$ represent the pseudo emotion-evoking mask (refer to Sec. 4.1) and predicted emotion-evoking mask, respectively.

For emotional explanation, we use a cross-entropy loss as the language loss to generate emotion explanations:

$$L_{\text{lang}} = L_{\text{XE}}(\mathcal{X}, \widehat{\mathcal{X}}), \quad (6)$$

Our model is trained by minimizing the sum of all losses:

$$L_{\text{total}} = L_{\text{mask}} + L_{\text{lang}}. \quad (7)$$

¹In the field of image captioning, both the GT caption and the image are provided as input during training, whereas during inference, only the image is used as input.

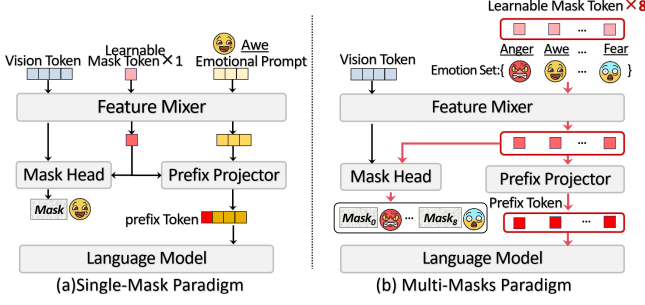


Figure 4: Our proposed framework supports two paradigms. (a) “Single-Mask” is our default paradigm with a single emotional mask output. (b) “Multi-Masks” enables the simultaneous generation of multiple emotion tokens masks for each image. It incorporates 8 learnable mask tokens, with each token corresponding to an emotion category in the emotion set.

3.5 Different Emotion Paradigms

In this paper, we consider two emotional segmentation paradigms: 1) The “**Single-Mask**” paradigm is to generate a single emotion-evoking mask based on an emotional prompt e “generate the mask for the emotion $_$ ” with a fixed emotion. It has already been introduced in Fig. 2. 2) Inspired by the observation that individuals may perceive distinct emotions from different regions of an image, we introduce a “**Multi-Masks**” paradigm to simulate the perception of multiple individuals simultaneously, which can process multiple masks for different emotions concurrently, enhancing segmentation flexibility. As illustrated in Fig. 4 (b), we extend the learnable mask token to 8 tokens $[m_0, \dots, m_7]$, each corresponding to one emotion from emotion set: {“amusement”, “awe”, “contentment”, “excitement”, “anger”, “disgust”, “fear”, “sadness”}. Then, $[m_0, \dots, m_7]$ along with the vision token v are fed into the feature mixer, where mask tokens-based self-attention and two cross-attentions in the reverse direction (mask tokens-to-vision token and vice-versa) are performed. Subsequently, the updated mask token m'_i and vision token v' are then passed through the mask head to obtain the predicted masks. The process is formulated as:

$$\begin{cases} [m'_0, \dots, m'_7], v' = \text{FeatureMixer}([m_0, \dots, m_7], v) \\ \widehat{\mathcal{M}}_i = \text{MaskHead}(m'_i, v'), i \in \{0, \dots, 7\} \end{cases}, \quad (8)$$

where $\widehat{\mathcal{M}}_i$ is the predicted emotion-evoking mask for the i -th emotion category. Compared to the Single-Mask paradigm, the eight specific learnable mask tokens allow the model to more effectively segment distinct emotions. This hypothesis has been validated experimentally (see Tab. 6).

For explanation generation, we map the updated mask token m'_i to the corresponding prefix token f_i through the prefix projector, where $i \in \{0, \dots, 7\}$. Then, as described in Sec. 3.3, we use the language model to generate emotional explanations:

$$\begin{cases} f_i = \text{PrefixProjector}(m'_i), i \in \{0, \dots, 7\} \\ \widehat{\mathcal{X}}_i = \text{LanguageModel}(v, [f_i, \mathcal{X}_i]) \end{cases}, \quad (9)$$

where $\mathcal{X}_i / \widehat{\mathcal{X}}_i$ denotes the ground-truth / predicted explanation for the i -th emotion category. During training, the training objective

of Multi-Masks paradigm is implemented using Eq. 10, which is the similar as that of Single-Mask paradigm:

$$L_{total} = \sum_{emo=0}^7 L_{mask}^{emo} + \sum_{emo=0}^7 L_{lang}^{emo}. \quad (10)$$

4 Experiments

4.1 Experimental Setup

Datasets. Due to the high cost of pixel-level annotation, the largest available dataset for art emotion understanding, ArtEmis[1], does not include mask annotations. Specifically, it consists of 80,031 artworks paired with 454,684 affective responses accompanied by explanatory utterances, with an {85%/5%/15%} split for training/validation/testing. We use the training set of ArtEmis for explanation training, and for segmentation training, we adopt a *weakly supervised strategy* to generate pseudo pixel-level mask labels for training (**Training dataset**). Following [6], we utilize VinVL [56] to detect candidate proposal regions for each image, and use CLIP [40] to compute the similarity between each region and the corresponding emotion-related explanatory utterances. The resulting similarity maps are treated as pseudo emotion-evoking masks, which serve as supervisory signals for training the emotion segmentation model.

The APOLO dataset [6] is an emotion-stimuli dataset that provides manually annotated emotion-evoking masks for the validation and test sets of the ArtEmis dataset [1]. Specifically, It contains 6,781 emotion-evoking masks for 4,718 artworks across 8 emotions, with corresponding explanatory utterances for each emotion-evoking mask. The dataset is divided into validation and test sets, with a 20%/80% of split. In this study, APOLO is exclusively used for model evaluation (**Testing dataset**).

Evaluation metrics. For **emotional segmentation**, we consider bounding box [39] and segmentation [13] scenarios as in [6]. For both scenarios, we calculate the precision with intersection over union (IoU) threshold θ ($\text{Pr}@_\theta$, including $\text{Pr}@_{25}$ and $\text{Pr}@_{50}$). For **explanation**, BLEU, METEOR, and ROUGE are used to evaluate the semantic relevance between generated explanations and GT explanations. And CLIPScore [18] is a reference-free metric to evaluate similarity between text and image. Furthermore, we use emotion-alignment (EA) [1] to measure whether the deduced emotion of explanation is aligned with the GT emotion of the mask.

Implementation Details. The feature dimension d_k of emotional prompt /learnable mask token is 256. For segmentation, the feature mixer includes $N = 2$ blocks. For explanation generation, we choose GPT-2 [45] as language model. It consists of $M = 6$ transformer blocks and 12 attention heads. In the cross attention of language model, following [45, 55], we use CLIP ViT-B/16 [40] to extract visual features with a dimensionality of 768. The word embedding dimension d_w is consistently set to 768. The explanations are truncated no longer than 25. **During training**, the parameters of both the visual encoder and the feature mixer are frozen. The total batch size is 16 via 4-step gradient accumulation with a per-step batch size of 4. We adopt the AdamW optimizer [16] for all trainable parameters. The learning rate for the language model is $2e-4$. For the Single-Mask paradigm, the emotion projector, mask head, and prefix projector are collectively assigned a learning rate of $1e-4$, whereas for the Multi-Masks paradigm, the learning rate is

Table 1: Method comparison on the APOLO test set. Emo-Rel is \checkmark when the model can generate stimulus masks related to a specific emotion. “-” indicates that this result is not available for this method. “*” indicates results reproduced by us. The best and second best numbers in each column are marked with bold font and underlined, respectively.

Method	Emo-Rel	Bounding Box		Segmentation		EA	BLEU ₁	BLEU ₂	BLEU ₃	BLEU ₄	METEOR	ROUGE-L	CLIPScore
		Pr@25	Pr@50	Pr@25	Pr@50								
Entire artwork	×	82.37	63.81	68.61	37.70	-	-	-	-	-	-	-	-
FasterRCNN	×	84.03	66.40	74.43	43.67	-	-	-	-	-	-	-	-
VinVL	×	84.43	67.54	75.10	43.94	-	-	-	-	-	-	-	-
CASNet	×	84.84	66.02	76.40	44.15	-	-	-	-	-	-	-	-
CASNet II	×	84.84	63.59	76.24	40.18	-	-	-	-	-	-	-	-
VilBERT	\checkmark	82.17	63.08	72.14	39.64	-	-	-	-	-	-	-	-
12-in-1	\checkmark	72.51	50.71	63.90	31.87	-	-	-	-	-	-	-	-
CLIP+VinVL	\checkmark	81.97	63.00	71.29	40.05	-	-	-	-	-	-	-	-
CLIP+SAM *	\checkmark	82.00	61.18	61.10	28.30	-	-	-	-	-	-	-	-
TRIS *	\checkmark	84.97	65.67	75.28	34.72	-	-	-	-	-	-	-	-
WESR	\checkmark	84.30	66.66	75.89	<u>44.97</u>	-	-	-	-	-	-	-	-
SCA _{base} *	\checkmark	<u>86.00</u>	<u>67.69</u>	<u>77.93</u>	44.62	<u>42.6</u>	<u>16.2</u>	<u>6.6</u>	<u>3.0</u>	<u>1.5</u>	<u>6.7</u>	<u>17.7</u>	<u>55.1</u>
EmoSEM (ours)	\checkmark	86.29	68.65	78.06	45.45	56.6	21.4	8.8	4.0	2.0	8.4	18.2	56.8

Table 2: Comparing EmoSEM with the baseline SCA_{base} and its high-configuration version SCA_{huge} after fine-tuning (denoted as SCA_{huge}-FT). Our model is highly competitive across most metrics, particularly in Pr@50 and EA, which are key indicators for segmentation and explanation task. Importantly, the number of parameters in our model is only 18.5% of that in SCA_{huge}-FT.

Method	#Params	Bounding Box		Segmentation		EA	BLEU ₁	BLEU ₂	BLEU ₃	BLEU ₄	METEOR	ROUGE-L	CLIPScore
		Pr@25	Pr@50	Pr@25	Pr@50								
SCA _{base} *	237.67M	<u>86.00</u>	67.69	77.93	44.62	42.6	16.2	6.6	3.0	1.5	6.7	17.7	55.1
SCA _{huge} -FT*	1499.21M	86.29	<u>68.13</u>	78.15	<u>44.99</u>	49.9	<u>19.3</u>	<u>8.3</u>	<u>3.9</u>	<u>1.9</u>	<u>8.2</u>	18.4	60.0
EmoSEM (ours)	276.62M	86.29	68.65	<u>78.06</u>	45.45	56.6	21.4	8.8	4.0	2.0	8.4	<u>18.2</u>	<u>56.8</u>

Table 3: Computational efficiency comparison of different models.

Model	Backbone	#Params	Training/Inference GPU	Training Time	FLOPs↓	Inference Speed↑
SCA _{base} *	SAM _{base} +GPT2	237.67M	1×RTX 4090	47h, 10 epochs	500.21G	5.91 (FPS)
SCA _{huge} -FT*	SAM _{huge} +GPT2 _{large}	1499.21M	1×RTX 4090	125h, 10 epochs	3018.16G	1.58 (FPS)
EmoSEM (ours)	SAM _{base} +GPT2	276.62M	1×RTX 4090	36h, 10 epochs	509.17G	6.11 (FPS)

set to $8e-5$. **During testing**, all segmentation visualizations in this paper use linear scaling to map the mask matrix to the image, and we use nucleus sampling [19] with a probability 0.9 for explanation prediction. For detailed computational costs, please refer to Tab. 3.

4.2 Main Evaluation

R1: How capable are existing segmentation models in detecting emotional stimuli? We benchmark our approach against existing artistic emotion segmentation methods, which are grouped into two types. The first group comprises methods that produce segmentation results without explicit emotional grounding, including full-image segmentation (Entire Artwork [6]), region proposal networks (Faster R-CNN [42], VinVL [56]), and saliency detection models (CASNet [13], CASNet II [12]). The second group contains

techniques that explicitly link regions to emotion category, exemplified by referring expressions models using emotion prompt as textual input (ViBERT [33], 12-in-1 [34], TRIS [31] reproduced by us), CLIP-based emotion-region similarity methods (CLIP+VinVL [6], CLIP+SAM reproduced by us), and a pixel-level emotion classification model trained with pseudo-labels (WESR [6]). As shown in Tab. 1, existing methods [12, 13, 31, 33, 34, 42, 56] perform sub-optimally on the emotional segmentation task. This suggests that objective segmentation models do not transfer well to the domain of emotion-oriented segmentation. Furthermore, our method surpasses WESR [6], e.g., in the segmentation scenario, achieving gains of 2.17% and 0.48% in Pr@25 and Pr@50, respectively.

R2: Can our model be effective in sentiment interpretation and segmentation? : Yes. For emotional segmentation, compared

Table 4: Ablation study of the prefix token. m'' and p'' represent mask prefix and emotional prompt prefix in Eq. 3, respectively.

Method	Prefix Token		Bounding Box		Segmentation		EA	BLEU ₁	BLEU ₂	BLEU ₃	BLEU ₄	METEOR	ROUGE-L	CLIPScore
	m''	p''	Pr@25	Pr@50	Pr@25	Pr@50								
#1	×	×	86.16	67.63	77.71	43.19	12.4	18.6	6.8	2.8	1.2	8.0	16.8	54.6
#2	✓	×	86.18	67.76	77.83	<u>44.68</u>	52.6	20.5	8.5	<u>3.6</u>	<u>1.8</u>	8.3	<u>17.7</u>	55.0
#3	×	✓	<u>86.23</u>	<u>67.95</u>	<u>77.91</u>	44.64	<u>52.8</u>	<u>21.3</u>	<u>8.7</u>	3.5	1.7	<u>8.4</u>	17.6	<u>56.2</u>
EmoSEM	✓	✓	86.29	68.65	78.06	45.45	56.6	21.4	8.8	4.0	2.0	8.4	18.2	56.8

Table 5: Ablation study of different mask prefix strategies. “Ambiguity-Aware” refers to concatenating multiple valid masks output by SAM to form the mask prefix for the language model, while “Ambiguity-Unaware” refers to using only one valid mask as the mask prefix.

Mask Prefix Strategy	Bounding Box		Segmentation		EA	BLEU ₁	BLEU ₂	BLEU ₃	BLEU ₄	METEOR	ROUGE-L	CLIPScore
	Pr@25	Pr@50	Pr@25	Pr@50								
Ambiguity-Aware	<u>86.23</u>	<u>68.22</u>	<u>77.95</u>	<u>45.15</u>	<u>55.6</u>	21.4	<u>8.6</u>	<u>3.8</u>	<u>1.8</u>	8.4	<u>17.8</u>	<u>56.3</u>
Ambiguity-Unaware	86.29	68.65	78.06	45.45	56.6	21.4	8.8	4.0	2.0	8.4	18.2	56.8

Table 6: Ablation study of different paradigms. “Single-Mask” is our default paradigm with a Single emotional Mask output (refer to Fig. 4(a)). “Multi-Masks” denotes the model enables the simultaneous generation of Multiple emotional Masks for each art image (refer to Fig. 4(b)). The proposed framework achieves superior performance under both paradigms.

Paradigm	Bounding box		Segmentation		EA	BLEU ₁	BLEU ₂	BLEU ₃	BLEU ₄	METEOR	ROUGE-L	CLIPScore
	Pr@25	Pr@50	Pr@25	Pr@50								
Single-Mask	86.29	<u>68.65</u>	<u>78.06</u>	<u>45.45</u>	56.6	<u>21.4</u>	<u>8.8</u>	4.0	2.0	<u>8.4</u>	18.2	56.8
Multi-Masks	<u>86.09</u>	68.98	78.13	46.68	<u>54.6</u>	22.2	9.0	4.0	<u>1.9</u>	8.7	18.2	<u>56.6</u>

to the state-of-the-art in Tab. 1, our method achieves superior performance across all metrics. For explanation generation, EmoSEM demonstrates significant advantages over the SCA_{base} , *e.g.*, achieving gains of 1.7% in METEOR. Most notably, it attains a 14.0% enhancement in emotion alignment (EA). These results validate EmoSEM’s dual capability in advancing both segmentation precision and emotional explanation quality.

R3: Comparison with the SCA_{huge} after fine-tuning. We fine-tune SCA_{huge} , which follows the framework in Fig. 3 (a), while it uses $SAM_{huge}+GPT2_{large}$ as its backbone and has been pretrained for captioning [20]. As shown in Tab. 2, our method achieves comparable performance compared with SCA_{huge} -FT (which has huge model parameters). In emotional segmentation, EmoSEM demonstrates competitive results with notable Pr@50 improvements of 0.52% (bounding box) and 0.46% (segmentation). Additionally, while maintaining similar semantic quality, EmoSEM significantly enhances EA score by 6.7%. Overall, these findings highlight its potential as a competitor to larger models in emotion understanding.

R4: Does the computational cost of the model provide an advantage? Yes. In Tab. 3, compared to SCA_{base} , our method introduces only minimal parameter overhead while achieving shorter training time and faster inference speed. In contrast to SCA_{huge} -FT, our model is only 18.5% of its size, with FLOPs reduced to 16.9%, training time shortened to 28.8%, and inference speed improved by 3.9 times. Combining the aforementioned emotion understanding

performance comparisons, our model has achieved a much better accuracy-efficiency trade-off.

4.3 Further Analysis

Here, we further evaluate the effectiveness of each proposed component, including the prefix token (R5), different mask prefix strategies (R6), fine-tuning design (R7), and different paradigms (R8).

R5: The effect of proposed prefix token. In Tab. 4, removing prefix token (#1) results in the worst performance, particularly in semantic metrics and EA, confirming that an independent language model struggles with effective pixel-level emotion understanding. Using either the mask prefix (#2) or the prompt prefix (#3) alone improves performance, with EA increasing by 40.2% and 40.4%, respectively. The best performance is achieved when both prefixes are combined, for example, a 2.26% improvement in Pr@50, a 0.8% increase in BLEU₄, and a 44.2% boost in EA compared to #1.

R6: Different mask prefix strategies. SAM can generate multiple candidate masks for ambiguous input (*i.e.*, Ambiguity-Aware strategy [23]). For simplicity, we can only use a default mask (*i.e.*, Ambiguity-UnAware strategy). Tab. 5 shows that when using multiple masks as mask prefixes (Ambiguity-Aware design), performance drops in most metrics, *e.g.*, decreasing by 1.0% in EA and 0.4% in ROUGE-L. We adopt the Ambiguity-UnAware setup.

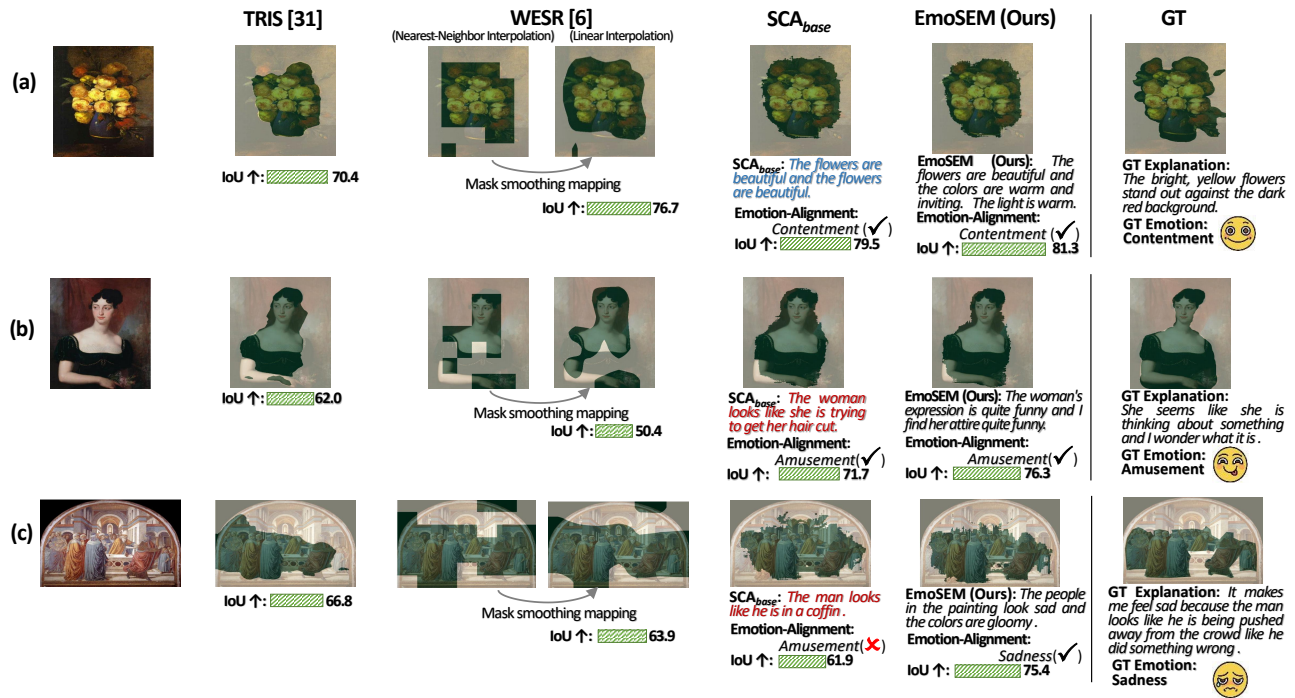


Figure 5: Examples comparing different methods on APOLO test set. We compare three methods, including TRIS [31], WESR [6], and the proposed baseline SCA_{base} based on SCA [20] for our task. Both TRIS and WESR perform more inaccurately in emotional segmentation than SCA_{base} and ours. In contrast, our method gives the best results. SCA_{base} generates more focused segmentation but struggles with emotional interpretation. The blue texts indicate influential explanations; red texts indicate large discrepancies between the semantics of explanations and visual content of mask. IoU is the intersection over union (IoU) of the predicted mask and the GT emotion-evoking mask, while the Emotion-Alignment metric [1] displays the most relevant emotion category aligned with the emotion of the explanations.

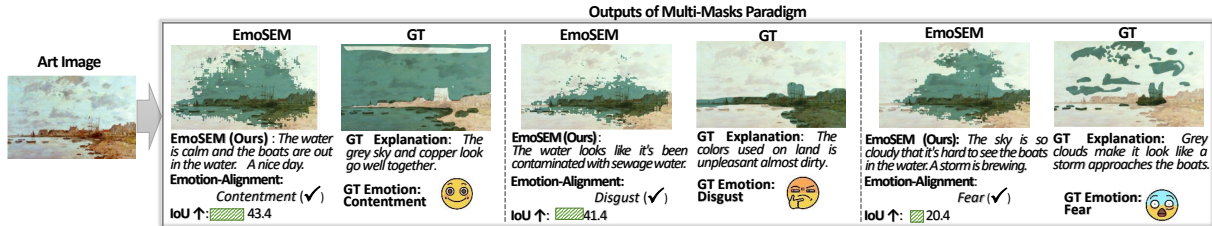


Figure 6: The visualization results of Multi-Masks paradigm. Our Multi-Masks paradigm can models the distinctive emotional experiences of diverse individuals in response to the same artistic image.

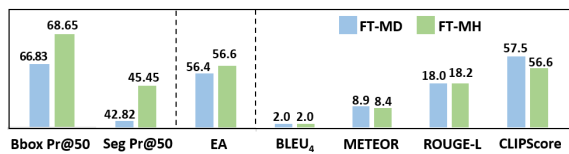


Figure 7: Fine-tuning strategies comparison. “FT-MD” means the entire mask decoder is fine-tuned, and “FT-MH” signifies that only the mask head is fine-tuned.

R7: The effect of fine-tuning design. Fig. 7 illustrates the performance from two fine-tuning strategies. The results indicate that fine-tuning the entire Mask Decoder (FT-MD) does not offer

obvious improvements in semantic metrics, and leads to a significant drop in segmentation performance, e.g., a decrease of 2.63% in segmentation Pr@50. Based on this finding, we adopt a strategy of fine-tuning only the mask head (FT-MH) in all experiments.

R8: Investigation of different paradigms. As shown in Tab. 6, both paradigms demonstrate robust performance, while some differences are observed. First, the Multi-Masks paradigm shows superior performance with Pr@50 improving by 0.33% and 1.23% in two scenarios. This improvement is attributed to the eight different mask tokens enabling more precise emotional segmentation learning (see Fig. 4(b)). Second, while both paradigms maintain

comparable semantic quality for explanation, the Single-Mask paradigm outperforms with a 2.0% higher EA score. This discrepancy might result from its explicit emotional prompt prefix p'' facilitating emotion-text alignment.

4.4 Qualitative Results

In this section, we comprehensively evaluate the model’s performance and summarize the following findings: 1) As shown in Fig. 5, our method achieves superior results, producing segments closest to the ground truth (GT) and generating more accurate emotional explanations. 2) In Fig. 8, our model can generate diverse emotional responses and interpretations for the same visual input, better reflecting the subjective nature of human emotion. 3) In Fig. 6, the Multi-Masks paradigm simultaneously generates regions and explanations for multiple emotions such as “contentment,” “disgust,” and “fear,” demonstrating the model’s capacity for multi-emotion understanding. 4) We also show the failure sample in Fig. 9. It is worth noting that although there are differences in segmentation accuracy (IoU=12.9), our explanation is semantically consistent with the predicted mask and correctly conveys the emotion of “Fear”. This suggests inaccurate results may arise from the inherent subjectivity of emotional segmentation. Future work should explore multi-dimensional evaluation frameworks that can recognize multiple emotional focal points.

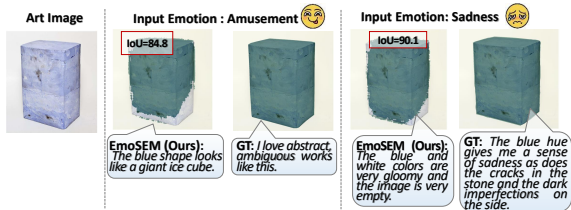


Figure 8: The same visual elicits different emotion responses.

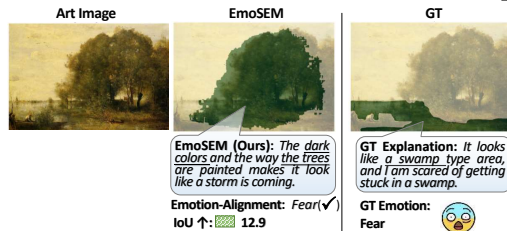


Figure 9: The failed cases.

5 Conclusion

This paper explores a novel and challenging task in the domain of artistic comprehension: emotional segmentation and explanation generation. To this end, we establish a representative baseline framework and propose a novel scheme, EmoSEM, which fills the research gap in emotion-oriented visual segmentation, realizes the cross-modal cognitive leap from pixel-level perception to emotion-level understanding. We conduct thorough evaluations across backbones of varying scales and give deep analyses. EmoSEM achieves state-of-the-art performance, demonstrating superior capabilities in both emotional localization and interpretation.

References

- [1] Panos Achlioptas, Maks Ovsjanikov, Kilichbek Haydarov, Mohamed Elhoseiny, and Leonidas J Guibas. 2021. Artemis: Affective language for visual art. In *CVPR*. 11569–11579.
- [2] Xavier Alameda-Pineda, Elisa Ricci, Yan Yan, and Nicu Sebe. 2016. Recognizing emotions from abstract paintings using non-linear matrix completion. In *Proceedings of the IEEE conference on computer vision and pattern recognition*. 5240–5248.
- [3] Jinglun Cen, Chunmei Qing, Haochun Ou, Xiangmin Xu, and Junpeng Tan. 2024. MASNNet: Multi-Aspect Semantic Auxiliary Network for Visual Sentiment Analysis. *IEEE TAC* (2024), 1–12.
- [4] Liang-Chieh Chen, George Papandreou, Iasonas Kokkinos, Kevin Murphy, and Alan L Yuille. 2017. Deeplab: Semantic image segmentation with deep convolutional nets, atrous convolution, and fully connected crfs. *IEEE transactions on pattern analysis and machine intelligence* 40, 4 (2017), 834–848.
- [5] Ming Chen, Lu Zhang, and Jan P Allebach. 2015. Learning deep features for image emotion classification. In *2015 IEEE International Conference on Image Processing (ICIP)*. IEEE, 4491–4495.
- [6] Tianwei Chen, Noa Garcia, Liangzhi Li, and Yuta Nakashima. 2024. Retrieving Emotional Stimuli in Artworks. In *Proceedings of the 2024 International Conference on Multimedia Retrieval*. 515–523.
- [7] Bowen Cheng, Ishan Misra, Alexander G Schwing, Alexander Kirillov, and Rohit Girdhar. 2022. Masked-attention mask transformer for universal image segmentation. In *Proceedings of the IEEE/CVF conference on computer vision and pattern recognition*. 1290–1299.
- [8] Simuo Deng, Lifang Wu, Ge Shi, Leahao Xing, Wenjin Hu, Heng Zhang, and Ye Xiang. 2022. Simple but powerful, a language-supervised method for image emotion classification. *IEEE Transactions on Affective Computing* 14, 4 (2022), 3317–3331.
- [9] Terry Diffey. 2014. *Tolstoy’s ‘What is Art?’*. Routledge.
- [10] Xiaoyi Dong, Jianmin Bao, Yinglin Zheng, Ting Zhang, Dongdong Chen, Hao Yang, Ming Zeng, Weiming Zhang, Lu Yuan, Dong Chen, et al. 2023. Maskclip: Masked self-distillation advances contrastive language-image pretraining. In *Proceedings of the IEEE/CVF Conference on Computer Vision and Pattern Recognition*. 10995–11005.
- [11] Alexey Dosovitskiy, Lucas Beyer, Alexander Kolesnikov, Dirk Weissenborn, Xiaohua Zhai, Thomas Unterthiner, Mostafa Dehghani, Matthias Minderer, G Heigold, S Gelly, et al. 2020. An Image is Worth 16x16 Words: Transformers for Image Recognition at Scale. In *International Conference on Learning Representations*.
- [12] Shaojing Fan, Zhiqi Shen, Ming Jiang, Bryan L Koenig, Mohan S Kankanhalli, and Qi Zhao. 2022. Emotional attention: From eye tracking to computational modeling. *IEEE Transactions on Pattern Analysis and Machine Intelligence* 45, 2 (2022), 1682–1699.
- [13] Shaojing Fan, Zhiqi Shen, Ming Jiang, Bryan L Koenig, Juan Xu, Mohan S Kankanhalli, and Qi Zhao. 2018. Emotional attention: A study of image sentiment and visual attention. In *Proceedings of the IEEE Conference on computer vision and pattern recognition*. 7521–7531.
- [14] Maujama Firdaus, Hardik Chauhan, Asif Ekbal, and Pushpak Bhattacharyya. 2020. EmoSen: Generating sentiment and emotion controlled responses in a multimodal dialogue system. *IEEE Transactions on Affective Computing* 13, 3 (2020), 1555–1566.
- [15] Golnaz Ghiasi, Xiuye Gu, Yin Cui, and Tsung-Yi Lin. 2022. Scaling open-vocabulary image segmentation with image-level labels. In *European conference on computer vision*. Springer, 540–557.
- [16] Sylvain Gugger and Jeremy Howard. 2018. Adamw and super-convergence is now the fastest way to train neural nets. *last accessed* 19 (2018).
- [17] Kaiming He, Xiangyu Zhang, Shaoqing Ren, and Jian Sun. 2016. Deep residual learning for image recognition. In *CVPR*. 770–778.
- [18] Jack Hessel, Ari Holtzman, Maxwell Forbes, Ronan Le Bras, and Yejin Choi. 2021. Clipscore: A reference-free evaluation metric for image captioning. *arXiv preprint arXiv:2104.08718* (2021).
- [19] Ari Holtzman, Jan Buys, Li Du, Maxwell Forbes, and Yejin Choi. 2019. The curious case of neural text degeneration. *arXiv preprint arXiv:1904.09751* (2019).
- [20] Xiaoke Huang, Jianfeng Wang, Yansong Tang, Zheng Zhang, Han Hu, Jiwen Lu, Lijuan Wang, and Zicheng Liu. 2024. Segment and caption anything. In *Proceedings of the IEEE/CVF conference on computer vision and pattern recognition*. 13405–13417.
- [21] William James. 1948. What is emotion? 1884. (1948).
- [22] Chao Jia, Yinfei Yang, Ye Xia, Yi-Ting Chen, Zarana Parekh, Hieu Pham, Quoc Le, Yun-Hsuan Sung, Zhen Li, and Tom Duerig. 2021. Scaling up visual and vision-language representation learning with noisy text supervision. In *International conference on machine learning*. PMLR, 4904–4916.
- [23] Alexander Kirillov, Eric Mintun, Nikhila Ravi, Hanzi Mao, Chloe Rolland, Laura Gustafson, Tete Xiao, Spencer Whitehead, Alexander C Berg, Wan-Yen Lo, et al. 2023. Segment anything. In *Proceedings of the IEEE/CVF international conference on computer vision*. 4015–4026.

- [24] Mengcheng Lan, Chaofeng Chen, Yiping Ke, Xinjiang Wang, Litong Feng, and Wayne Zhang. 2024. Proxyclip: Proxy attention improves clip for open-vocabulary segmentation. In *European Conference on Computer Vision*. Springer, 70–88.
- [25] Tong Li, Yunhui Hu, and Xinxiao Wu. 2021. Image captioning with inherent sentiment. In *ICME*, 1–6.
- [26] Xiangtai Li, Henghui Ding, Haobo Yuan, Wenwei Zhang, Jiangmiao Pang, Guangliang Cheng, Kai Chen, Ziwei Liu, and Chen Change Loy. 2024. Transformer-based visual segmentation: A survey. *IEEE transactions on pattern analysis and machine intelligence* (2024).
- [27] Zhuwen Li, Qifeng Chen, and Vladlen Koltun. 2018. Interactive image segmentation with latent diversity. In *Proceedings of the IEEE conference on computer vision and pattern recognition*. 577–585.
- [28] Feng Liang, Bichen Wu, Xiaoliang Dai, Kunpeng Li, Yinan Zhao, Hang Zhang, Peizhao Zhang, Peter Vajda, and Diana Marculescu. 2023. Open-vocabulary semantic segmentation with mask-adapted clip. In *Proceedings of the IEEE/CVF conference on computer vision and pattern recognition*. 7061–7070.
- [29] Tsung-Yi Lin, Priya Goyal, Ross Girshick, Kaiming He, and Piotr Dollár. 2017. Focal loss for dense object detection. In *Proceedings of the IEEE international conference on computer vision*. 2980–2988.
- [30] Chenxiao Liu, Zheyong Xie, Sirui Zhao, Jin Zhou, Tong Xu, Minglei Li, and Enhong Chen. 2024. Speak from heart: an emotion-guided LLM-based multimodal method for emotional dialogue generation. In *Proceedings of the 2024 International Conference on Multimedia Retrieval*. 533–542.
- [31] Fang Liu, Yuhao Liu, Yuqiu Kong, Ke Xu, Lihe Zhang, Baocai Yin, Gerhard Hancke, and Rynson Lau. 2023. Referring image segmentation using text supervision. In *Proceedings of the IEEE/CVF International Conference on Computer Vision*. 22124–22134.
- [32] Jonathan Long, Evan Shelhamer, and Trevor Darrell. 2015. Fully convolutional networks for semantic segmentation. In *Proceedings of the IEEE conference on computer vision and pattern recognition*. 3431–3440.
- [33] Jiaseen Lu, Dhruv Batra, Devi Parikh, and Stefan Lee. 2019. Vilbert: Pretraining task-agnostic visiolinguistic representations for vision-and-language tasks. *Advances in neural information processing systems* 32 (2019).
- [34] Jiaseen Lu, Vedanuj Goswami, Marcus Rohrbach, Devi Parikh, and Stefan Lee. 2020. 12-in-1: Multi-task vision and language representation learning. In *Proceedings of the IEEE/CVF conference on computer vision and pattern recognition*. 10437–10446.
- [35] Alexander Mathews, Lexing Xie, and Xuming He. 2016. Senticap: Generating image descriptions with sentiments. In *AAAI*, 1–7.
- [36] Fausto Milletari, Nassir Navab, and Seyed-Ahmad Ahmadi. 2016. V-net: Fully convolutional neural networks for volumetric medical image segmentation. In *2016 fourth international conference on 3D vision (3DV)*. Ieee, 565–571.
- [37] Youssef Mohamed, Faizan Farooq Khan, Kilichbek Haydarov, and Mohamed Elhoseiny. 2022. It is okay to not be okay: Overcoming emotional bias in affective image captioning by contrastive data collection. In *CVPR*. 21263–21272.
- [38] Saif Mohammad and Svetlana Kiritchenko. 2018. Wikiart emotions: An annotated dataset of emotions evoked by art. In *Proceedings of the eleventh international conference on language resources and evaluation (LREC 2018)*.
- [39] Kuan-Chuan Peng, Amir Sadovnik, Andrew Gallagher, and Tshuan Chen. 2016. Where do emotions come from? predicting the emotion stimuli map. In *2016 IEEE international conference on image processing (ICIP)*. IEEE, 614–618.
- [40] Alec Radford, Jong Wook Kim, Chris Hallacy, Aditya Ramesh, Gabriel Goh, Sandhini Agarwal, Girish Sastry, Amanda Askell, Pamela Mishkin, Jack Clark, et al. 2021. Learning transferable visual models from natural language supervision. In *International conference on machine learning*. PmlR, 8748–8763.
- [41] Alec Radford, Jeffrey Wu, Rewon Child, David Luan, Dario Amodei, Ilya Sutskever, et al. 2019. Language models are unsupervised multitask learners. *OpenAI blog* 1, 8 (2019), 9.
- [42] Shaoqing Ren, Kaiming He, Ross Girshick, and Jian Sun. 2015. Faster r-cnn: Towards real-time object detection with region proposal networks. *Advances in neural information processing systems* 28 (2015).
- [43] Jie Ruan, Yue Wu, Xiaojun Wan, and Yuesheng Zhu. 2024. Describe images in a boring way: Towards cross-modal sarcasm generation. In *Proceedings of the IEEE/CVF Winter Conference on Applications of Computer Vision*. 5701–5710.
- [44] Olga Russakovsky, Jia Deng, Hao Su, Jonathan Krause, Sanjeev Satheesh, Sean Ma, Zhiheng Huang, Andrej Karpathy, Aditya Khosla, Michael Bernstein, et al. 2015. Imagenet large scale visual recognition challenge. *International journal of computer vision* 115 (2015), 211–252.
- [45] Victor Sanh, Lysandre Debut, Julien Chaumond, and Thomas Wolf. 2019. DistilBERT, a distilled version of BERT: smaller, faster, cheaper and lighter. *arXiv preprint arXiv:1910.01108* (2019).
- [46] Xiangheng Shan, Dongyue Wu, Guilin Zhu, Yuanjie Shao, Nong Sang, and Changxin Gao. 2024. Open-vocabulary semantic segmentation with image embedding balancing. In *Proceedings of the IEEE/CVF Conference on Computer Vision and Pattern Recognition*. 28412–28421.
- [47] Karen Simonyan and Andrew Zisserman. 2014. Very deep convolutional networks for large-scale image recognition. *arXiv preprint arXiv:1409.1556* (2014).
- [48] Ashish Vaswani, Noam Shazeer, Niki Parmar, Jakob Uszkoreit, Llion Jones, Aidan N Gomez, Lukasz Kaiser, and Illia Polosukhin. 2017. Attention is all you need. *Advances in neural information processing systems* 30 (2017).
- [49] Xinxiao Wu and Tong Li. 2023. Sentimental Visual Captioning using Multimodal Transformer. *IJCV* 131, 4 (2023), 1073–1090.
- [50] Enze Xie, Wenhai Wang, Zhiding Yu, Anima Anandkumar, Jose M Alvarez, and Ping Luo. 2021. SegFormer: Simple and efficient design for semantic segmentation with transformers. *Advances in neural information processing systems* 34 (2021), 12077–12090.
- [51] Mengde Xu, Zheng Zhang, Fangyun Wei, Han Hu, and Xiang Bai. 2023. SAN: side adapter network for open-vocabulary semantic segmentation. *IEEE Transactions on Pattern Analysis and Machine Intelligence* 45, 12 (2023), 15546–15561.
- [52] Ning Xu, Brian Price, Scott Cohen, Jimei Yang, and Thomas S Huang. 2016. Deep interactive object selection. In *Proceedings of the IEEE conference on computer vision and pattern recognition*. 373–381.
- [53] Jingyuan Yang, Jie Li, Leida Li, Xiumei Wang, Yuxuan Ding, and Xinbo Gao. 2022. Seeking subjectivity in visual emotion distribution learning. *IEEE Transactions on Image Processing* 31 (2022), 5189–5202.
- [54] Jufeng Yang, Dongyu She, and Ming Sun. 2017. Joint Image Emotion Classification and Distribution Learning via Deep Convolutional Neural Network.. In *IJCAL*. 3266–3272.
- [55] Jing Zhang, Liang Zheng, Meng Wang, and Dan Guo. 2024. Training a small emotional vision language model for visual art comprehension. In *European Conference on Computer Vision*. Springer, 397–413.
- [56] Pengchuan Zhang, Xiujun Li, Xiaowei Hu, Jianwei Yang, Lei Zhang, Lijuan Wang, Yejin Choi, and Jianfeng Gao. 2021. Vinvl: Revisiting visual representations in vision-language models. In *Proceedings of the IEEE/CVF conference on computer vision and pattern recognition*. 5579–5588.
- [57] Wentian Zhao, Xinxiao Wu, and Xiaoxun Zhang. 2020. Memcap: Memorizing style knowledge for image captioning. In *AAAI*. 12984–12992.
- [58] Yian Zhao, Kehan Li, Zesen Cheng, Pengchong Qiao, Xiawu Zheng, Rongrong Ji, Chang Liu, Li Yuan, and Jie Chen. 2024. GraCo: Granularity-controllable interactive segmentation. In *Proceedings of the IEEE/CVF Conference on Computer Vision and Pattern Recognition*. 3501–3510.
- [59] Sixiao Zheng, Jiachen Lu, Hengshuang Zhao, Xiatian Zhu, Zekun Luo, Yabiao Wang, Yanwei Fu, Jianfeng Feng, Tao Xiang, Philip HS Torr, et al. 2021. Re-thinking semantic segmentation from a sequence-to-sequence perspective with transformers. In *Proceedings of the IEEE/CVF conference on computer vision and pattern recognition*. 6881–6890.
- [60] Ying Zhou, Hui Xue, and Xin Geng. 2015. Emotion distribution recognition from facial expressions. In *Proceedings of the 23rd ACM international conference on Multimedia*. 1247–1250.